Lamellae from Rods | Hot Paper

DOI: 10.1002/ange.201404089

"Raft" Formation by Two-Dimensional Self-Assembly of Block Copolymer Rod Micelles in Aqueous Solution**

Georgios Rizis, Theo G. M. van de Ven, and Adi Eisenberg**

Abstract: *Block copolymers can form a broad range of self-assembled aggregates. In solution, planar assemblies usually form closed structures such as vesicles; thus, free-standing sheet formation can be challenging. While most polymer single crystals are planar, their growth usually occurs by uptake of individual chains. Here we report a novel lamella formation mechanism: core-crystalline spherical micelles link up to form rods in solution, which then associate to yield planar arrays. For the system of poly(ethylene oxide)-block-polycaprolactone in water, co-assembly with homopolycaprolactone can induce a series of morphological changes that yield either rods or lamellae. The underlying lamella formation mechanism was elucidated by electron microscopy, while light scattering was used to probe the kinetics. The hierarchical growth of lamellae from one-dimensional rod subunits, which had been formed from spherical assemblies, is novel and controllable in terms of product size and aspect ratio.*

Block copolymers containing both soluble and insoluble moieties can self-assemble in the presence of a selective solvent.[1] The micelle-like structures thereby obtained are morphologically diverse, and are central to a range of advanced applications in nanotechnology.[2] Further innovation in structure design requires control strategies for self-assembly across multiple length scales to produce anisotropic, patterned or hierarchical materials. Noteworthy advances have been made through "living" crystallization-driven self-assembly, where complex yet highly uniform aggregates could be achieved.[3] Recent work indicates that poly(ethylene oxide)-*block*-polycaprolactone (PEO-*b*-PCL) assemblies can also be controlled morphologically through the crystallinity of the PCL block.[4] In pure water, however, this system exhibits generally slow dynamics, such that the latter effects are usually mild.

[*] Dr. G. Rizis, Prof. T. G. M. van de Ven, Prof. A. Eisenberg
McGill University
801 Sherbrooke St. West, Montreal, H3A 0B8, Quebec (Canada)
E-mail: theo.vandeven@mcgill.ca
adi.eisenberg@mcgill.ca

[**] We thank the Fonds Québécois de la Recherche sur la Nature et les Technologies (FQRNT), the Centre for Self-Assembled Chemical Structures (CSACS), and the National Sciences and Engineering Research Council of Canada (NSERC) Discovery grant for financial support. Thanks are also due for the block copolymer sample PEO_{45}-*b*-PCL_{18}, which had been prepared by Dr. Tony Azzam in connection with earlier work.

Supporting information for this article (synthetic protocols and sample preparation details, along with additional characterization data) is available on the WWW under http://dx.doi.org/10.1002/anie.201404089.

Here we show that the influence of crystallinity in the PEO-*b*-PCL system can be enhanced significantly by the inclusion of PCL homopolymer into the micelle core, yielding extended sheets that are akin to chain-folded crystalline lamellae. The average sizes and aspect ratios of the products depend on the amount of homo-PCL added during micellization, offering easy access to multiple structures. An overview of the latter approach is provided first, but emphasis is placed on the underlying self-assembly mechanism which, to our knowledge, has not been encountered before. Structures form by a sequence of directional adhesion events, consisting of linear aggregation of spheres to yield rods, followed by the planar alignment of rods to form the lamellae. The rod subunits are roughly equal in length to the lamellae, much like the wooden logs in a raft. The novelty of this "raft" formation mechanism emerges by comparison not only to other examples in polymer science, but across a much wider spectrum of self-assembled two-dimensional (2D) structures. Some known strategies to organize materials in 2D include the exfoliation of layered solids,[5] oriented attachment and mesocrystal formation,[6] subunit pre-organization,[7] and supramolecular chemistry.[8] While research in 2D self-assembly is diverse, we are unaware of any example where highly elongated subunits (aspect ratio > 50) align spontaneously to form large yet discrete lamellae without help from a foreign interface.

To prepare the micelles for this study, both the block copolymer and the homo-PCL chains were co-dissolved in dioxane, followed by the addition of water as a selective precipitant for the PCL. Results obtained with two copolymers are described; these materials contain a constant PEO_{45} block (subscripts give the number average of repeat units) attached to hydrophobic blocks of either PCL_{18} or PCL_{24}. The best results were obtained by using the homopolymer PCL_{10}, which does not alter the initial spherical morphology under the conditions examined here. Fresh spheres exhibit diameters of 20–30 nm, as determined by dynamic light scattering (DLS) and transmission electron microscopy (TEM); typical results are shown in the supporting information (Figure S1 in the Supporting Information (SI)). These spheres were also freeze-dried and then analyzed calorimetrically (see Table S1 in SI).

Upon storage in water, spheres form higher-order structures with time, the shape of which depends on the amount of homo-PCL used during assembly. From rods, to thin strips, to much wider lamellae, the system is biased gradually towards 2D growth rather than linear association as the homo-PCL content increases, as illustrated in Figure 1. The transformation rates increase with PCL_{10} content, which indicates further its destabilizing effect on the spheres (see Figure S2 in SI). For

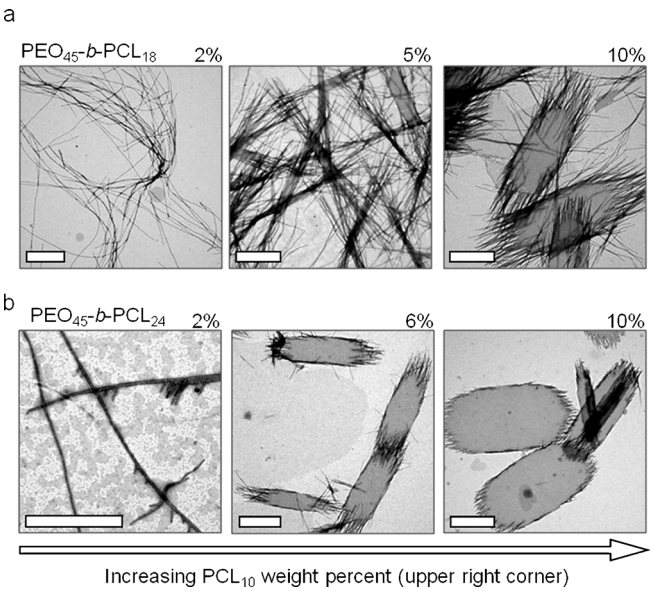

Figure 1. Morphological transformations induced by incorporation of PCL_{10}. TEM images show products obtained in samples of a) PEO_{45}-*b*-PCL_{18} and b) PEO_{45}-*b*-PCL_{24} as a function of PCL_{10} content (increasing left to right). Scale bar: 2 μm.

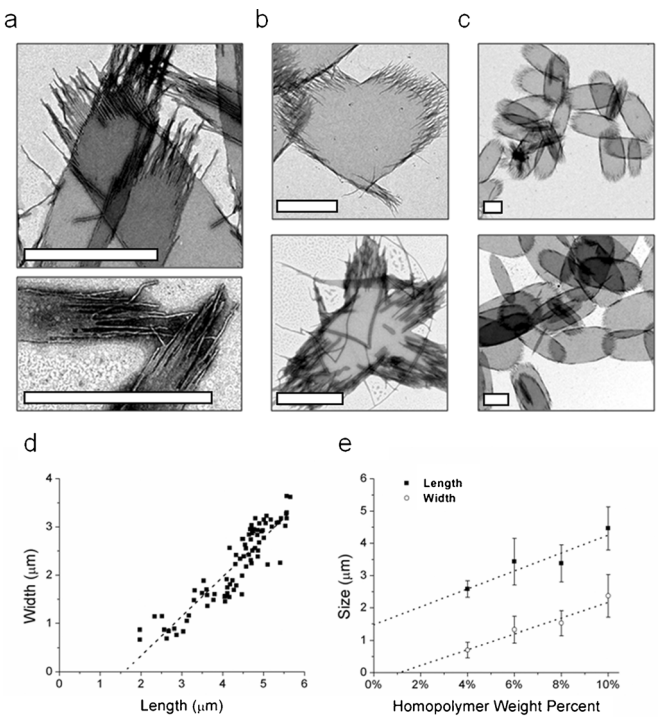

Figure 2. Structural features of PEO-*b*-PCL "rafts." Typical TEM images showing a) details of both smooth and fringed edges, b) examples of crystallographic twinning (note the recurrence of 60° and 120° angles), and c) collection of "raft"-type lamellae. d) Correlation between length and width of individual lamellae in samples of PEO_{45}-*b*-PCL_{24} containing 10% (w/w) PCL_{10}; the sample composition is the same as for Figure 2c. e) Average lengths and widths of lamellae of PEO_{45}-*b*-PCL_{24} as a function of PCL_{10} content; error bars represent the standard deviation. Scale bar: 2 μm.

spheres of equal homopolymer-to-block copolymer weight ratio, the final product is the same regardless of the total polymer concentration in water (see Figure S3 in SI); formation rates, however, vary linearly with concentration, as we reported previously for homopolymer-free PEO-*b*-PCL spheres.[4c] The latter findings suggest that changes occurring within isolated micelle cores may determine the overall behavior.

The homopolymer effect is also latent in the present system, in contrast to immediate effects seen elsewhere.[9] Alone, PCL_{10} does not produce the same structures in water, but aggregates to form heterogeneous clusters instead; the material is entirely hydrophobic, and much smaller amounts than present in the micellar samples just described yield turbid solutions. If a solution of PCL_{10} in dioxane is added to pre-formed spheres of PEO-*b*-PCL in water, the system also does not yield lamellae and is rendered turbid instantly. Besides globular clusters, TEM images reveal that 1D structures also abound (see Figure S4 in SI). Perhaps the post-assembly addition of PCL_{10} mediates adhesion between spheres to some extent, in this case with a 1D bias. As similar results were shown in another core-crystalline system, the phenomenon may be quite common.[9c] Crucially, however, these samples do not evolve beyond the stage of long strips, suggesting that the two polymeric components must be co-assembled initially in order to form "rafts".

In reconstructing the steps involved in "raft" formation, we highlight certain features of the lamellar products. First, the rod-like fibrils emerge only at the opposing narrow edges, while the longer edges appear smooth. As illustrated in Figure 2a, the long edges of the lamellae exhibit no structural defects due to single sphere vacancies, as would be expected if the lamellae were grown directly from the spheres without the rods serving as intermediates. A subset of the lamellae exhibit apparent twinning, which produces heart-shaped aggregates (example shown in Figure 2b). Twinning occurs at angles of roughly 60° or 120°, which is consistent with the hexagonal shape known for PEO-*b*-PCL single crystals.[10] It is worth mentioning that similar twinning behavior also exists in inorganic nanoparticle systems.[11] Structures are not always symmetric about the axis associated with twinning, and some lamellae contain more than one of these axes. Other side-products include rods which bend repeatedly at sharp angles (ca. 60°), and additional structures shown in the supporting information (see Figure S5 in SI). For twinned lamellae, the absence of imperfections along the twinning axis, and lack of a clearly distinguishable rod in the central region, is noteworthy. It suggests that it may not be the rod ends that align along the twinning axis, but kinks present in the rods (see Figure S5 in SI for images of kinked rods).

A closer look reveals that the lengths and widths of individual lamellae are proportional. Qualitatively, this feature is seen in TEM images of large numbers of lamellae, such as those shown in Figure 2c. One example of this length-width relation is shown in Figure 2d, in which the fringe lengths were excluded from the measurements. Although the lamellae are polydisperse in size, their aspect ratio is predictable based on this relation. Notably, extrapolation of this graph to zero width yields a finite length; the relation

varies somewhat with sample composition, and lengths between 0.8 μm and 1.6 μm are obtained as the width approaches zero (see Table S2 in the supporting information). Thus, within any given sample, the narrowest possible lamella, as extrapolated in this manner, describes a rod micelle.

Despite the broad size distribution, the average lamella sizes vary with homo-PCL content, as shown in Figure 2e with a series of isochronally-aged samples. Even though only lamellae are considered, the graph provides valuable insight on morphological trends from rods to lamellae. For instance, the average predicted width is zero as the PCL_{10} content approaches values below 1.3% (w/w), which predicts accurately that homopolymer-free samples contain rods rather than lamellae, whereas samples containing 2% (w/w) PCL_{10} can develop small fringed lamellae (see Figure S6 in the supporting information). At zero PCL_{10} content, length values extrapolate to 1.6 μm in Figure 2e, which is in agreement with the lengths of rods found in homopolymer-free samples.

The involvement of rods in lamella formation is also apparent in the early stages of sample evolution: the system does not seem to produce lamellae without first having formed rods. TEM images of rods formed within a period of hours following self-assembly, which exhibit a tendency to associate laterally and to coalesce, are shown in Figure S7 in the Supporting Information. In DLS experiments, rod formation is reflected in the appearance of a secondary slow-diffusing mode; only later are even larger modes observed, which reflect lamella formation. To verify whether lamellae were being formed directly from spheres, the samples were filtered through a narrow-pore membrane, which isolates the spherical micelle fraction from samples in the midst of the transition. After the large species were removed, the remaining spheres did, indeed, form rods, from which new lamellae were produced only later (see Figure S7 and S8 in SI).

The co-existence of rods and polydisperse lamellae within individual samples suggests that the system probably does not initiate growth in a synchronous fashion. In fact, new "rafts" seem to be forming while in the presence of other full-sized products, which is also consistent with the ability of filtered samples to form more "rafts". Thus, intermediates can be found alongside the "rafts" in most samples, as shown in Figure 3a. These oligomeric structures seem to resist dissociation and transfer of cylindrical units to the larger crystalline species. Moreover, it is remarkable that the growth of lamellae formed at early times does not dominate the transformation profile, and no evidence suggests that lamellae keep growing to macroscopic sizes. If the samples are filtered at a stage where changes start slowing down, conveniently, the intermediates persist for longer periods, facilitating their characterization; images of aligned rods, partially fused together in 2D, are shown in Figure 3b. Notably, these images, which were obtained in isochronal samples containing increasing amounts of PCL_{10}, also resemble a hypothetical sequence describing the growth a "raft" with time: First, laterally adhesive rods come together to form oligomers, matching rod lengths in order to maximize overlap. Once the rods are fused together, the assembly becomes irreversible. Finally, the "raft" can continue to grow by uptake of more rods along the edges, provided that their lengths are comparable. As a result, while the association of spheres in 1D controls the length of the "rafts", their width is regulated independently by the 1D aggregation of aligned rods.

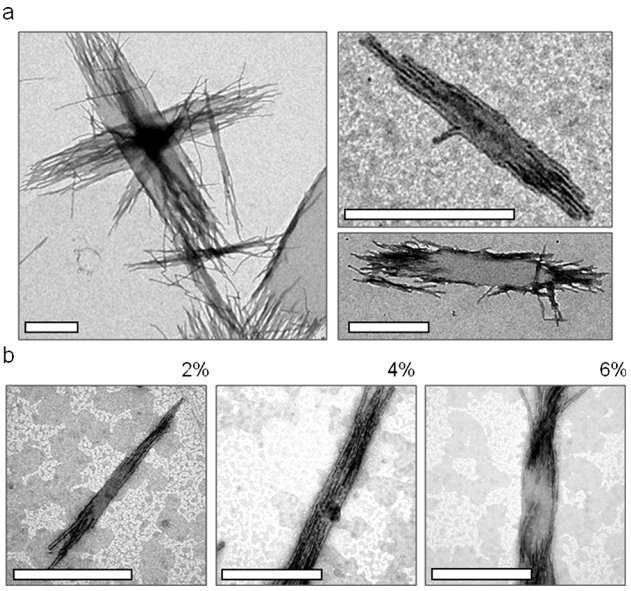

Figure 3. Intermediates in the formation of PEO-*b*-PCL "rafts". a) TEM images showing oligomeric structures as well as rod subunits, both free and bundled, which co-exist with larger lamellar aggregates. b) TEM images of small lamellar structures found in filtered micelles of PEO_{45}-b-PCL_{24} containing PCL_{10} (amount listed above each image). The samples were aged for 2 days before imaging. Scale bar: 1 μm.

Prior examples of free-standing PEO-*b*-PCL lamellae of comparable sizes are limited to solution-grown single crystals in organic media.[10] To show how such crystals are related to the self-assembled "rafts", we grew crystals without PCL_{10} in *n*-hexanol through a protocol inspired by the original studies. A typical TEM image of the products is shown in Figure 4a. By sedimentation, these lamellar crystals were then transferred into water where, as illustrated in Figure 4b, they developed fringed edges and also released rod-like fragments. These distortions may be caused by the expansion of PEO coils in water from a compact state in *n*-hexanol.[10b] Note that the fragmentation mirrors, in reverse, the associative steps of "raft" formation: in the micellar samples, linear structures are formed first, which then align and fuse together in parallel; the inverse sequence seems to occur as crystals formed in *n*-hexanol fall apart in water, perhaps due to preferential fracture lines in the crystal. Lacking the growth history associated with "rafts", the recrystallized products release rod-like segments of various sizes in water, many of which are branched (see Figure S9 in SI). Note that these crystals do not fragment completely, suggesting that PCL_{10} is not necessary to maintain their integrity in water. However, only by co-assembly with homo-PCL can lamellar crystals actually form directly in water from these particular copolymers.

In summary, a novel mechanism of lamella formation, involving the 2D alignment of block copolymer rod micelles, is described. This new mechanism is involved in generating the morphological continuum that becomes easily accessible for a single copolymer sample by using homopolymer chains.

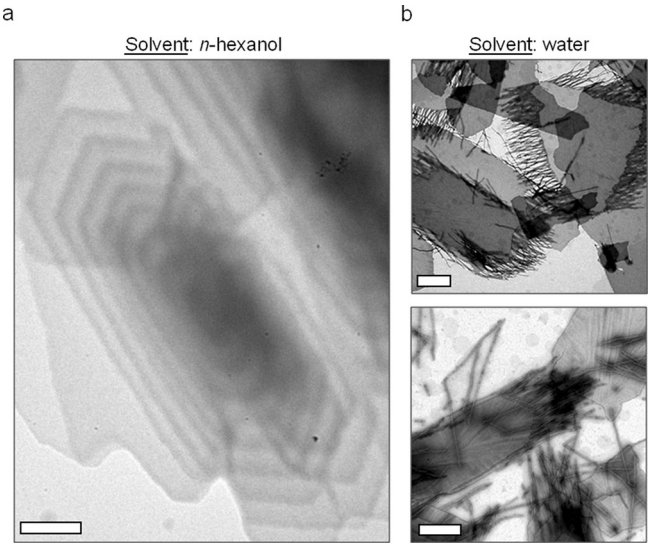

Figure 4. Block copolymer crystals grown in organic media. Samples shown were prepared from PEO_{45}-*b*-PCL_{24}; see Figure S9 in the Supporting Information for examples of PEO_{45}-*b*-PCL_{18} crystals. a) TEM images of lamellar crystals of grown and cast from *n*-hexanol suspensions. These images depict the original state of the crystals, which then fragment in water. b) TEM images of the fragmented products. Note the alignment of cylindrical features emanating from the lamellar crystals. Scale bar: 1 μm.

The unique feature here is the evolution of dimensionality in a sequence of 1D assembly steps: sphere aggregation provides the building blocks for growth along an orthogonal direction. The rods align and, thus, determine the size of the final 2D product.

Received: April 8, 2014
Published online: July 2, 2014

Keywords: block copolymers · hierarchical self-assembly · lamellae · polymer crystallinity · rod micelles

[1] a) A. Qin, M. Tian, C. Ramireddy, S. E. Webber, P. Munk, Z. Tuzar, *Macromolecules* **1994**, *27*, 120–126; b) L. Zhang, A. Eisenberg, *Science* **1995**, *268*, 1728–1731; c) *Amphiphilic Block Copolymers: Self-Assembly and Applications* (Eds.: P. Alexandridis, B. Lindman), Elsevier, New York, **2000**; d) S. Jain, F. S. Bates, *Science* **2003**, *300*, 460–464; e) Y. Mai, A. Eisenberg, *Chem. Soc. Rev.* **2012**, *41*, 5969–5985.

[2] a) Z. B. Li, M. A. Hillmyer, T. P. Lodge, *Langmuir* **2006**, *22*, 9409–9417; b) H. Cui, Z. Chen, S. Zhong, K. L. Wooley, D. J. Pochan, *Science* **2007**, *317*, 647–650; c) D. A. Christian, A. W. Tian, W. G. Ellenbroek, I. Levental, K. Rajagopal, P. A. Janmey, A. J. Liu, T. Baumgart, D. E. Discher, *Nat. Mater.* **2009**, *8*, 843–849; d) G. Liu, I. Wyman in *Complex Macromolecular Architectures: Synthesis Characterization and Self-Assembly* (Eds.: N. Hadjichristidis, A. Hirao, Y. Tezuka, F. Du Prez), Wiley, Singapore, **2011**, pp. 739–761; e) F. S. Bates, M. A. Hillmyer, T. P. Lodge, C. M. Bates, K. T. Delaney, G. H. Fredrickson, *Science* **2012**, *336*, 434–440; f) A. H. Gröschel, F. H. Schacher, H. Schmalz, O. V. Borisov, E. B. Zhulina, A. Walther, A. H. Muller, *Nat. Commun.* **2012**, *3*, 710.

[3] a) X. Wang, G. Guerin, H. Wang, Y. Wang, I. Manners, M. A. Winnik, *Science* **2007**, *317*, 644–647; b) T. Gädt, N. S. Ieong, G. Cambridge, M. A. Winnik, I. Manners, *Nat. Mater.* **2009**, *8*, 144–150; c) J. B. Gilroy, T. Gadt, G. R. Whittell, L. Chabanne, J. M. Mitchels, R. M. Richardson, M. A. Winnik, I. Manners, *Nat. Chem.* **2010**, *2*, 566–570; d) P. A. Rupar, L. Chabanne, M. A. Winnik, I. Manners, *Science* **2012**, *337*, 559–562; e) A. M. Mihut, J. J. Crassous, H. Schmalz, M. Drechsler, M. Ballauff, *Soft Matter* **2012**, *8*, 3163; f) J. Schmelz, F. H. Schacher, H. Schmalz, *Soft Matter* **2013**, *9*, 2101–2107; g) N. Petzetakis, A. P. Dove, R. K. O'Reilly, *Chem. Sci.* **2011**, *2*, 955; h) J. Schmelz, M. Karg, T. Hellweg, H. Schmalz, *ACS Nano* **2011**, *5*, 9523–9534.

[4] a) Z. X. Du, J. T. Xu, Z. Q. Fan, *Macromolecules* **2007**, *40*, 7633–7637; b) K. Rajagopal, A. Mahmud, D. A. Christian, J. D. Pajerowski, A. E. Brown, S. M. Loverde, D. E. Discher, *Macromolecules* **2010**, *43*, 9736–9746; c) G. Rizis, T. G. M. van de Ven, A. Eisenberg, *Soft Matter* **2014**, *10*, 2825–2835.

[5] a) K. S. Novoselov, A. K. Geim, S. V. Morozov, D. Jiang, Y. Zhang, S. V. Dubonos, I. V. Grigorieva, A. A. Firsov, *Science* **2004**, *306*, 666–669; b) G. Battaglia, A. J. Ryan, *Nat. Mater.* **2005**, *4*, 869–876.

[6] a) C. Schliehe, B. H. Juarez, M. Pelletier, S. Jander, D. Greshnykh, M. Nagel, A. Meyer, S. Foerster, A. Kornowski, C. Klinke, H. Weller, *Science* **2010**, *329*, 550–553; b) M. Li, H. Schnablegger, S. Mann, *Nature* **1999**, *402*, 393–395; c) Z. Tang, Z. Zhang, Y. Wang, S. C. Glotzer, N. A. Kotov, *Science* **2006**, *314*, 274–278; d) H. S. Park, A. Agarwal, N. A. Kotov, O. D. Lavrentovich, *Langmuir* **2008**, *24*, 13833–13837; e) N. A. Kotov, S. Srivastava, *Soft Matter* **2009**, *5*, 1146–1156; f) H. Cölfen, M. Antonietti, *Angew. Chem.* **2005**, *117*, 5714–5730; *Angew. Chem. Int. Ed.* **2005**, *44*, 5576–5591.

[7] a) S. Zhang, T. Holmes, C. Lockshin, A. Rich, *Proc. Natl. Acad. Sci. USA* **1993**, *90*, 3334–3338; b) K. T. Nam, S. A. Shelby, P. H. Choi, A. B. Marciel, R. Chen, L. Tan, T. K. Chu, R. A. Mesch, B. C. Lee, M. D. Connolly, C. Kisielowski, R. N. Zuckermann, *Nat. Mater.* **2010**, *9*, 454–460; c) U. B. Sleytr, P. Messner, D. Pum, M. Sara, *Angew. Chem.* **1999**, *111*, 1098–1120; *Angew. Chem. Int. Ed.* **1999**, *38*, 1034–1054; d) K. M. M. Carneiro, N. Avakyan, H. F. Sleiman, *Wiley Interdiscip. Rev. Nanomed. Nanobiotechnol.* **2013**, *5*, 266–285.

[8] a) S. I. Stupp, S. Son, H. C. Lin, L. S. Li, *Science* **1993**, *259*, 59–63; b) H. Cui, T. Muraoka, A. G. Cheetham, S. I. Stupp, *Nano Lett.* **2009**, *9*, 945–951; c) Y. Kubo, Y. Kitada, R. Wakabayashi, T. Kishida, M. Ayabe, K. Kaneko, M. Takeuchi, S. Shinkai, *Angew. Chem.* **2006**, *118*, 1578–1583; *Angew. Chem. Int. Ed.* **2006**, *45*, 1548–1553; d) M. Numata, S. Shinkai, *Chem. Commun.* **2011**, *47*, 1961–1975; e) P. Kissel, R. Erni, W. B. Schweizer, M. D. Rossell, B. T. King, T. Bauer, S. Gotzinger, A. D. Schluter, J. Sakamoto, *Nat. Chem.* **2012**, *4*, 287–291; f) X. Zhang, D. Gorl, V. Stepanenko, F. Wurthner, *Angew. Chem.* **2014**, *126*, 1294–1298; *Angew. Chem. Int. Ed.* **2014**, *53*, 1270–1274.

[9] a) L. F. Zhang, A. Eisenberg, *J. Polym. Sci. Part B* **1999**, *37*, 1469–1484; b) M. Lazzari, D. Scalarone, C. E. Hoppe, C. Vazquez-Vazquez, M. A. Lopez-Quintela, *Chem. Mater.* **2007**, *19*, 5818–5820; c) S. F. Mohd Yusoff, J. B. Gilroy, G. Cambridge, M. A. Winnik, I. Manners, *J. Am. Chem. Soc.* **2011**, *133*, 11220–11230.

[10] a) J. R. Sun, X. S. Chen, C. L. He, X. B. Jing, *Macromolecules* **2006**, *39*, 3717–3719; b) R. M. Van Horn, J. X. Zheng, H.-J. Sun, M.-S. Hsiao, W.-B. Zhang, X.-H. Dong, J. Xu, E. L. Thomas, B. Lotz, S. Z. D. Cheng, *Macromolecules* **2010**, *43*, 6113–6119.

[11] Z. Y. Tang, Y. Wang, S. Shanbhag, M. Giersig, N. A. Kotov, *J. Am. Chem. Soc.* **2006**, *128*, 6730–6736.

